Plasmon polaritons in photonic metamaterial Fibonacci superlattices

E. Reyes-Gómez,[1] N. Raigoza,[1] S. B. Cavalcanti,[2] C. A. A. de Carvalho,[3,4] and L. E. Oliveira[4,5]
[1]*Instituto de Física, Universidad de Antioquia, Medellín AA 1226, Colombia*
[2]*Instituto de Física, UFAL–Cidade Universitária, Maceió 57072-970, AL, Brazil*
[3]*Instituto de Física, UFRJ, Rio de Janeiro 21945-972, RJ, Brazil*
[4]*Inmetro, Campus de Xerém, Duque de Caxias 25250-020, RJ, Brazil*
[5]*Instituto de Física, UNICAMP, CP 6165, Campinas 13083-970, SP, Brazil*
(Received 26 December 2009; revised manuscript received 2 March 2010; published 5 April 2010)

We study the properties of plasmon polaritons in one-dimensional photonic metamaterial superlattices resulting from the periodic repetition of a Fibonacci structure. We assume the system made up of positive refraction and metamaterial layers. A Drude-type dispersive response for both the dielectric permittivity and magnetic permeability of the left-handed material is considered. Maxwell's equations are solved for oblique incidence by using the transfer-matrix formalism. Our results show that the plasmon-polariton modes are considerably affected by the increasing of the Fibonacci-sequence order of the elementary cell. The loss of the long-range spatial coherence of the electromagnetic field along the growth direction, which is due to the quasiperiodicity of the elementary cell, leads to the splitting of the plasmon-polariton frequencies, resulting in a Cantor-type frequency spectra. Moreover, the calculated photonic dispersion indicates that if the plasma frequency is chosen within the photonic $\langle n(\omega)\rangle=0$ gap then the plasmon-polariton modes behave essentially as pure plasmon modes.

DOI: 10.1103/PhysRevB.81.153101 PACS number(s): 42.70.Qs, 41.20.Jb, 42.70.Gi, 78.20.Bh

The control and manipulation of light, as well as the study of its interaction with condensed matter, have been the subject of considerable amount of work in the last few decades. Photonic crystals (PCs) (Refs. 1–3) have emerged as a new class of optical materials displaying exciting and useful properties of practical application. Apart from the purely physical interest for investigating PCs, an additional motivation for studying them is provided by the challenge of constructing all-optical devices eventually capable of replacing electronic transistors.[4,5]

The advent of metamaterials, i.e., optical materials with negative index of refraction[6,7] theoretically described by Veselago[8] at the end of the 1960s, has opened up new interesting possibilities for studying PCs. In this context, one-dimensional (1D) periodic and quasiperiodic PCs made up of materials with positive and negative indices of refraction have been studied both from the experimental[9] and theoretical[10–12] points of view. Such systems display a band gap associated to the condition $\langle n\rangle=0$ (null average of the refractive index), which is essentially invariant with scaling.[13,14] Furthermore, at the interface between the metamaterial and the positive-refraction material, resonant interactions may take place between electromagnetic waves and an electronic plasma at the surface of the metamaterial, leading to electromagnetic surface waves known as surface-plasmon polaritons.[15]

Recent work has explored the possibility of exciting bulk plasmon polaritons along the growth direction in 1D periodic photonic superlattices containing a metamaterial.[16] For oblique incidence, as the magnetic (electric) field corresponding to TE (TM) modes has a nonvanishing component along the superlattice growth direction, such a field leads to the excitation of coupled bulk magnetic (electric) plasmon-polariton modes.[16]

The present study is concerned with the properties of plasmon polaritons in 1D photonic Fibonacci superlattices containing layers of metamaterial. We have focused in a 1D structure made up by using two different building blocks (layers) A and B, with width, electric permittivity, and magnetic permeability given by a and b, ϵ_A and ϵ_B, and μ_A and μ_B, respectively. We consider such a structure as periodic, with the elementary cell composed by the mth generation of the Fibonacci sequence, which is obtained from the recursion relation $S_m(A,B)=S_{m-1}(A,B)S_{m-2}(A,B)(m\geq 2)$, and the initial conditions $S_0(A,B)=B$ and $S_1(A,B)=A$. The Fibonacci sequence S_m may alternatively be obtained by substituting $B\rightarrow A$ and $A\rightarrow AB$ in S_{m-1}, i.e., through the inflation law $S_m(A,B)=S_{m-1}(AB,A)$. In addition, it is possible to show that $S_m(A,B)=S_{m-k}[S_{k+1}(A,B),S_k(A,B)]$, where $m\geq 2$ and $0\leq k\leq m$. The total number of elements (A and B) in the elementary cell S_m satisfies the Fibonacci succession, which may be recursively defined as $F_m=F_{m-1}+F_{m-2}$, with the initial conditions $F_0=F_1=1$. The ratio $\tau_m=F_{m+1}/F_m$ converges toward to the golden mean $\tau=(1+\sqrt{2})/2$, as m increases, and the length L_m of the elementary cell S_m may be obtained as $L_m=F_{m-1}a+F_{m-2}b$.

If the growth direction is taken along the z axis, the equation describing the electric-field amplitude E associated with the monochromatic TE modes (electric field parallel to the interface planes) propagating along the photonic superlattice is given by

$$\frac{d}{dz}\frac{1}{\mu(z)}\frac{d}{dz}E(z)=-\epsilon(z)\left[\frac{\omega^2}{c^2}-\frac{q^2}{n^2(z)}\right]E(z), \qquad (1)$$

where $n(z)=\sqrt{\mu(z)}\sqrt{\epsilon(z)}$, $\mu(z)$ and $\epsilon(z)$ are the position-dependent refraction index, magnetic permeability, and dielectric permittivity of the 1D system, respectively. At the interfaces, the vector function

$$\Psi(z) = \begin{pmatrix} E(z) \\ \frac{1}{\mu(z)} \frac{d}{dz} E(z) \end{pmatrix} \tag{2}$$

is a continuous function. Because of the periodicity of the 1D system, Ψ is an eigenfunction of the translation operator $\hat{T}_{L_m}$ across the length of the elementary cell S_m, and therefore

$$\hat{T}_{L_m} \Psi(0) = \Psi(L_m) = e^{ikL_m} \Psi(0). \tag{3}$$

In addition, one may define the transfer matrix $\mathbb{T}_m$ as the 2×2 matrix which connects the function Ψ at the beginning ($z=0$) and at the end ($z=L_m$) of the elementary cell S_m, i.e.,

$$\Psi(L_m) = \mathbb{T}_m \Psi(0). \tag{4}$$

Combining Eqs. (3) and (4), one may note that

$$[\mathbb{T}_m - e^{ikL_m} \mathbb{I}] \Psi(0) = 0, \tag{5}$$

where $\mathbb{I}$ is the 2×2 identity matrix. In other words, e^{ikL_m} and $\Psi(0)$ are the eigenvalues and eigenfunctions of the transfer matrix, respectively, whereas $\mathbb{T}_m$ is the matrix representation of the translation operator $\hat{T}_{L_m}$. From Eqs. (4) and (5)

$$\cos(kL_m) = R_m, \tag{6}$$

where R_m is the semitrace of $\mathbb{T}_m$, which is used to obtain the dispersion relations $\omega = \omega(k)$ [or $\nu = \nu(k)$, with $\nu = \omega/2\pi$] of the TE modes in the photonic superlattice. According to the rule for generating the Fibonacci sequence of order m, it is possible to see that $\mathbb{T}_m = \mathbb{T}_{m-2}\mathbb{T}_{m-1}$, and therefore[17] $R_m = 2R_{m-1}R_{m-2} - R_{m-3}$. In order to compute the semitrace R_m for a given value of $m > 2$, it is only necessary to known the semitraces R_0, R_1, and R_2. A simple calculation leads to

$$R_0 = \cos(Q_B b), \tag{7}$$

$$R_1 = \cos(Q_A a) \tag{8}$$

and

$$R_2 = \cos(Q_A a)\cos(Q_B b) - \frac{1}{2}\left[\frac{Q_A \mu_B}{Q_B \mu_A} + \frac{Q_B \mu_A}{Q_A \mu_B}\right] \sin(Q_A a)\sin(Q_B b), \tag{9}$$

where $Q_{A,B} = \sqrt{\frac{\omega^2}{c^2} n_{A,B}^2 - q^2}$ and $n_{A,B} = \sqrt{\mu_{A,B}}\sqrt{\epsilon_{A,B}}$ are the wave vector of the electromagnetic wave and the refraction index in the optical medium A or B, respectively. The wave vector q along the plane perpendicular to the growth direction may be given, according to Snell's law, as $q = n_A \sin(\theta_A) = n_B \sin(\theta_B)$, where θ_A and θ_B are the incidence angles in media A and B, respectively. We note that the TM modes may also be studied from Eqs. (6)–(9) but by replacing μ_A and μ_B by ϵ_A and ϵ_B, respectively, in Eq. (9). In the present work, we have denoted $\theta_A = \theta$, and chosen $\mu_A = \epsilon_A = 1$ in medium A, whereas in the metamaterial medium B we have taken Drude-type dispersive responses given by[18]

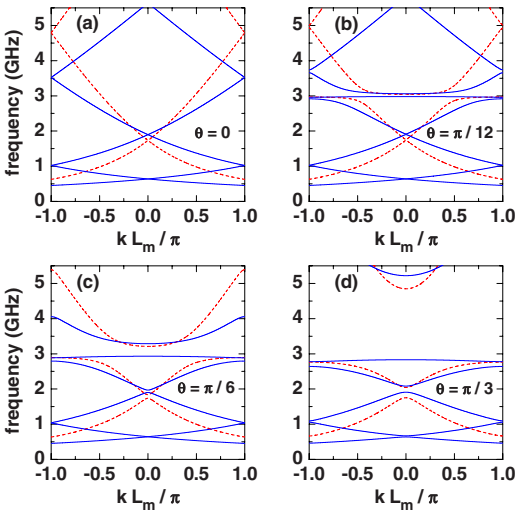

FIG. 1. (Color online) TE dispersion relation $\nu = \nu(k)$ in photonic Fibonacci superlattices with the elementary cell given by a Fibonacci sequence S_m (of length L_m), for different values of the incidence angle θ. Calculations were performed for air as slab A ($\epsilon_A = 1$ and $\mu_A = 1$), $a = b = 12$ mm, and $\omega_e/2\pi = \omega_m/2\pi = 3$ GHz for the Drude model in slab B. Dashed and solid lines correspond to the S_3 and S_4 Fibonacci generations in the elementary cell, respectively.

$$\epsilon_B(\omega) = \epsilon_0 - \frac{\omega_e^2}{\omega^2}, \quad \mu_B(\omega) = \mu_0 - \frac{\omega_m^2}{\omega^2}. \tag{10}$$

The frequencies associated to the electric and magnetic plasmon modes are $\nu_e = \frac{\omega_e}{2\pi\sqrt{\epsilon_0}}$ and $\nu_m = \frac{\omega_m}{2\pi\sqrt{\mu_0}}$, respectively. For the sake of simplicity, we have used $\epsilon_0 = 1$ and $\mu_0 = 1$ in the numerical results.

Figure 1 displays the dispersion relation $\nu = \nu(k)$, for different values of the incidence angle θ, in photonic superlattices with elementary cells given by the Fibonacci sequences S_3 and S_4. Present numerical results were obtained for $a = b = 12$ mm, and $\omega_e/2\pi = \omega_m/2\pi = 3$ GHz [cf. Eq. (10)]. Dashed and solid lines correspond to $m = 3$ and $m = 4$, respectively, where m is the order of the Fibonacci sequence used as the elementary cell of the superlattice. One may note that for normal incidence ($\theta = 0$) the non-Bragg $\langle n \rangle_m = 0$ frequency gaps are null, as one might expect[12] from the fact that $\langle \epsilon \rangle_m = \langle \mu \rangle_m = 0$, where $\langle \epsilon \rangle_m = (F_{m-1}\epsilon_A a + F_{m-2}\epsilon_B b)/L_m$ and $\langle \mu \rangle_m = (F_{m-1}\mu_A a + F_{m-2}\mu_B b)/L_m$. An increase in θ leads to non-Bragg gaps associated to $\langle n \rangle_m = 0$ and to the plasmon polariton gap.[16] In the case of plasmon polaritons, for normal incidence there is no component of the electric and magnetic field along the growth direction, and therefore no longitudinal plasmon polaritons are observed. For oblique incidence, however, the magnetic field corresponding to the TE modes has a nonvanishing component along the z-growth direction, which results in the excitation of longitudinal magnetic plasmon-polariton waves. One may note from Fig. 1 that, for oblique incidence, there exists one coupled mode for $m = 3$ and two coupled modes for $m = 4$. The number of excited plasmon-polariton modes corresponds to the number of metamaterial layers B (F_{m-2}) in the elementary cell S_m, as one may see from Fig. 2. The single plasmon-polariton sub-

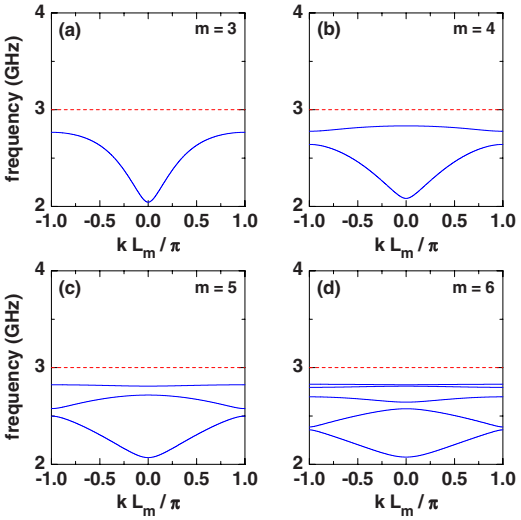

FIG. 2. (Color online) TE dispersion relation $\nu=\nu(k)$, in the vicinity of the magnetic plasmon frequency (dashed lines), for various values of the Fibonacci order m and for the incidence angle $\theta=\pi/3$. Parameters were taken as in Fig. 1. The number of plasmon polariton modes is just F_{m-2}.

band for $m=3$ splits into F_{m-2} plasmon-polariton subbands for a given value of $m>3$, a fact which is a consequence of the loss of the long-range spatial coherence of the electromagnetic field along superlattice axis due to the quasiperiodicity of the unit cell.

The dispersion relations in photonic superlattices with elementary cells given by the Fibonacci sequences S_3 and S_4 are displayed in Fig. 3 for various values of the incidence angle. Calculations were performed for $a=b=12$ mm, $\omega_e/2\pi=3$ GHz, and $\omega_m/2\pi=1$ GHz. One may note that the magnetic plasmon frequency $\frac{\omega_m}{2\pi\sqrt{\mu_0}}$ is within the non-Bragg $\langle n\rangle_m=0$ gap for $\theta=0$ (normal incidence). An increase in the incidence angle leads to a nearly flat plasmon-polariton dispersion inside the $\langle n\rangle_m=0$ gap. Such plasmon-polariton subbands behave essentially as pure bulk plasmon modes. The

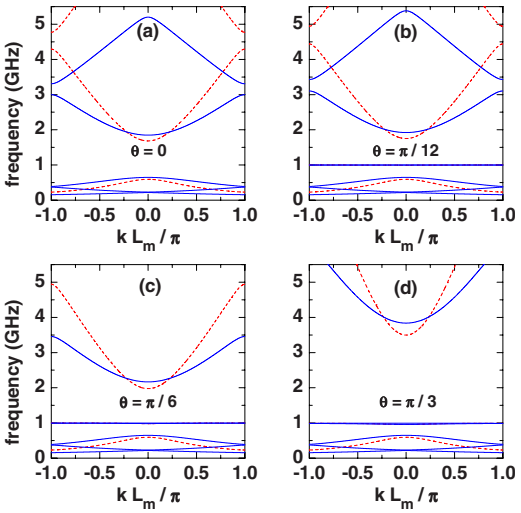

FIG. 3. (Color online) As in Fig. 1 with $\omega_e/2\pi=3$ GHz and $\omega_m/2\pi=1$ GHz.

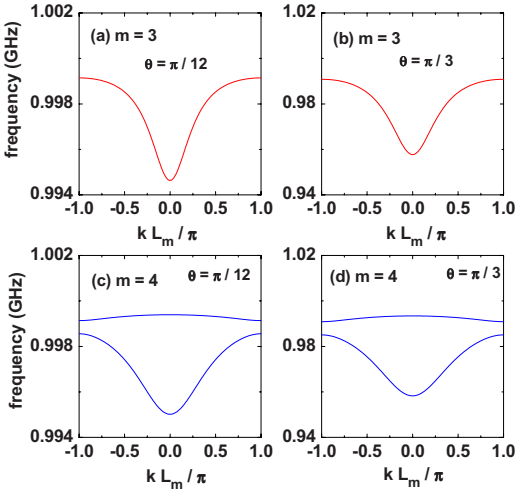

FIG. 4. (Color online) TE plasmon-polariton dispersion relations in photonic superlattices for two different values of incidence angle and order m of the Fibonacci sequence in the elementary cell. Calculations were performed for $a=b=12$ mm, and for plasma frequencies $\omega_e/2\pi=3$ GHz and $\omega_m/2\pi=1$ GHz.

plasmon-polariton subbands obtained for the elementary cells S_3 and S_4 in the superlattice system, and displayed in Figs. 3(b) and 3(d), respectively, are magnified for clarity in Fig. 4. Once more, it is clearly seen that the number of plasmon-polariton subbands are different for different values of the Fibonacci-sequence order of the elementary cell. In fact, for $m=3$ and $m=4$ the number of plasmon-polariton subbands are 1 and 2, respectively. Generally speaking, the number of plasmon-polariton modes in the photonic superlattice containing a Fibonacci sequence S_m in the elementary cell is F_{m-2}, which corresponds to the number of B-metamaterial layers in S_m (each of the F_{m-2} slabs B contributes to the whole spectra with a single bulk plasmon polariton).

If $a \gg b$, the distance between the different slabs B is so large that the corresponding plasmon polaritons do not interact. Such a situation leads to a F_{m-2}-degenerate plasmon-polariton subband in the superlattice system. If $a \sim b$, the spatial proximity between the metamaterial slabs breaks up such a degeneracy, leading to F_{m-2} different plasmon-polariton subbands. This behavior, which has already been observed for electron states in similar semiconductor systems,[19,20] is displayed in Fig. 5, which exhibits the evolution of the magnetic plasmon-polariton band structures of photonic superlattices as functions of the order of the Fibonacci sequence in the elementary cell, for two different values of the incidence angle. Numerical results were computed for $a=b=12$ mm, $\omega_e/2\pi=3$ GHz, and $\omega_m/2\pi=1$ GHz. From a physical point of view, the Cantor-type behavior of the plasmon-polariton subbands is due to the loss of long-range spatial coherence of the electromagnetic modes in the system caused by the quasiperiodicity of the elementary cell S_m. As an additional illustration, Fig. 6 exhibits the various plasmon-polariton bandwidths of photonic superlattices as functions of the incidence angle, for different values on the order m of the Fibonacci sequence in the elementary cell. Needless to say, all the results discussed

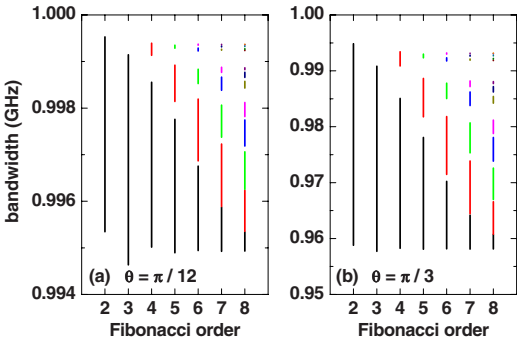

FIG. 5. (Color online) TE plasmon-polariton band structures of photonic superlattices, for two different values of the incidence angle, as functions of the order m of the Fibonacci sequence in the elementary cell. Results were obtained for $a=b=12$ mm, $\omega_e/2\pi=3$ GHz, and $\omega_m/2\pi=1$ GHz.

here for TE modes have a similar counterpart for TM modes.

To summarize, we have studied the properties of plasmon polaritons in 1D photonic superlattices in which Fibonacci sequences S_m play the role of elementary cells. We have shown that the properties of the plasmon polaritons in such systems strongly depend on the Fibonacci-sequence order m. If the plasmon frequency is an allowed frequency for normal incidence, the number of plasmon-polariton modes appearing for oblique incidence is just the number of metamaterial layers contained in S_m, and they correspond to the strong coupling of photons and plasmons. On the other hand, if the plasmon frequency lies within the $\langle n(\omega)\rangle=0$ gap, the number of plasmon-polariton subbands is also F_{m-2}, but the light-plasmon coupling weakens considerably, resulting in essentially dispersionless plasmonlike subbands, with their frequency spectra behaving as a Cantor-type set. Finally, we do hope that the present study on magnetic/electric plasmon-polariton modes will be useful for future experimental work

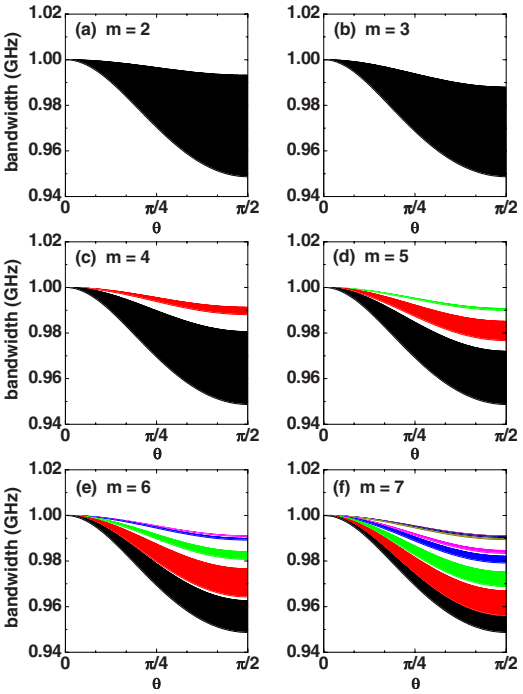

FIG. 6. (Color online) TE plasmon-polariton bandwidth of photonic superlattices, as functions of the incidence angle, for different values of the order m of the Fibonacci sequence in the elementary cell. Parameters used in numerical calculations were taken as in Fig. 5.

aimed at exploring the interplay between photonics and magnetism at nanoscales.

We would like to thank the Brazilian Agencies CNPq, FAPESP, FAPERJ, and FUJB, the Colombian Agency COLCIENCIAS, and CODI—University of Antioquia for partial financial support.

[1] E. Yablonovitch, Phys. Rev. Lett. **58**, 2059 (1987).
[2] S. John, Phys. Rev. Lett. **58**, 2486 (1987).
[3] S. G. Johnson and J. D. Joannopoulos, Acta Mater. **51**, 5823 (2003).
[4] N. Mattiucci, G. D'Aguanno, M. Scalora, and M. J. Bloemer, Appl. Phys. B: Lasers Opt. **81**, 389 (2005).
[5] M. F. Yanik, S. Fan, M. Soljačić, and J. D. Joannopoulos, Opt. Lett. **28**, 2506 (2003).
[6] J. B. Pendry, A. J. Holden, W. J. Stewart, and I. Youngs, Phys. Rev. Lett. **76**, 4773 (1996).
[7] J. B. Pendry, A. J. Holden, D. J. Robbins, and W. J. Steward, IEEE Trans. Microwave Theory Tech. **47**, 2075 (1999).
[8] V. G. Veselago, Sov. Phys. Usp. **10**, 509 (1968).
[9] L. Zhang, Y. Zhang, L. He, Z. Wang, H. Li, and H. Chen, J. Phys. D **40**, 2579 (2007).
[10] W. J. Hsueh, C. T. Chen, and C. H. Chen, Phys. Rev. A **78**, 013836 (2008).
[11] S. B. Cavalcanti, M. deDios-Leyva, E. Reyes-Gómez, and L. E. Oliveira, Phys. Rev. E **75**, 026607 (2007).
[12] A. Bruno-Alfonso, E. Reyes-Gómez, S. B. Cavalcanti, and L. E. Oliveira, Phys. Rev. A **78**, 035801 (2008).
[13] J. Li, L. Zhou, C. T. Chan, and P. Sheng, Phys. Rev. Lett. **90**, 083901 (2003).
[14] H. Jiang, H. Chen, H. Li, Y. Zhang, and S. Zhu, Appl. Phys. Lett. **83**, 5386 (2003).
[15] M. Dragoman and D. Dragoman, Prog. Quantum Electron. **32**, 1 (2008).
[16] E. Reyes-Gómez, D. Mogilevtsev, S. B. Cavalcanti, C. A. A. de Carvalho, and L. E. Oliveira, EPL **88**, 24002 (2009).
[17] M. Kohmoto, L. P. Kadanoff, and C. Tang, Phys. Rev. Lett. **50**, 1870 (1983).
[18] J. Pacheco, Jr., T. M. Grzegorczyk, B.-I. Wu, Y. Zhang, and J. A. Kong, Phys. Rev. Lett. **89**, 257401 (2002); G. V. Eleftheriades, A. K. Iyer, and P. C. Kremer, IEEE Trans. Microwave Theory Tech. **50**, 2702 (2002); A. Grbic and G. V. Eleftheriades, J. Appl. Phys. **92**, 5930 (2002); L. Liu, C. Caloz, C. C. Chang, and T. Itoh, *ibid.* **92**, 5560 (2002).
[19] F. Laruelle, D. Paquet, M. C. Joncour, B. Jusserand, J. Barrau, F. Mollot, and B. Etienne, in *Localization and Confinement of Electrons in Semiconductors*, Springer Series in Solid State Science Vol. 97, edited by F. Kuchar, H. Heinrich, and G. Bauer (Springer, Berlin, 1990), p. 258.
[20] F. Laruelle, B. Etienne, J. Barrau, K. Khirouni, J. C. Brabant, T. Amand, and M. Brouseau, Surf. Sci. **228**, 92 (1990).